Pacific-Atlantic Ocean influence on wildfires in northeast China (1774 to 2010)

Qichao Yao[1,2] (iD), Peter M. Brown[3] (iD), Shirong Liu[4], Monique E. Rocca[5] (iD), Valerie Trouet[2] (iD), Ben Zheng[6], Haonan Chen[7] (iD), Yinchao Li[8] (iD), Duanyang Liu[9], and Xiaochun Wang[1,10] (iD)

[1]College of Forestry, Northeast Forestry University, Harbin, China, [2]Laboratory of Tree-Ring Research, University of Arizona, Tucson, Arizona, USA, [3]Rocky Mountain Tree-Ring Research, Fort Collins, Colorado, USA, [4]Institute of Forest Ecology, Environment and Protection, Chinese Academy of Forestry, Beijing, China, [5]Ecosystem Science and Sustainability, Natural Resource Ecology Laboratory, Colorado State University, Fort Collins, Colorado, USA, [6]Department of Statistics, Colorado State University, Fort Collins, Colorado, USA, [7]Department of Electrical and Computer Engineering, Colorado State University, Fort Collins, Colorado, USA, [8]School of Remote Sensing and Information Engineering, Wuhan University, Wuhan, China, [9]Jiangsu Meteorological Observatory, Nanjing, China, [10]Harvard Forest, Harvard University, Petersham, Massachusetts, USA

Abstract Identification of effects that climate teleconnections, such as El Niño–Southern Oscillation (ENSO), Pacific Decadal Oscillation (PDO), and North Atlantic Oscillation (NAO), have on wildfires is difficult because of short and incomplete records in many areas of the world. We developed the first multicentury wildfire chronologies for northeast China from fire-scarred trees. Regional wildfires occurred every 7 years from the 1700s to 1947, after which fire suppression policies were implemented. Regional wildfires occurred predominately during drought years and were associated with positive phases of ENSO and PDO and negative NAO. Twentieth century meteorological records show that this contingent combination of +ENSO/+PDO/−NAO is linked to low humidity, low precipitation, and high temperature during or before late spring fire seasons. Climate and wildfires in northeast China may be predictable based on teleconnection phases, although future wildfires may be more severe due to effects of climate change and the legacy of fire suppression.

1. Introduction

Wildfire is in many ecosystems a central organizing disturbance process, affecting biogeochemical cycles, biodiversity and ecosystem structures, and hydrological processes [*Bowman et al.*, 2009]. Wildfire also often has profound social and economic impacts, which are forecast to increase with future intensification of human land use and anthropogenic climate change [*Moritz et al.*, 2014; *Abatzoglou and Williams*, 2016]. Increased wildfire sizes and severities in recent decades in many locations around the world have focused attention on potentially severe consequences of warmer temperatures, changes in rainfall patterns, earlier spring snow melt, and longer fire seasons [*Westerling et al.*, 2006; *Liu et al.*, 2010; *Jolly et al.*, 2015]. The occurrence, spread, and intensity of any single wildfire is mainly dependent on weather patterns that vary on daily to monthly time scales [*Flannigan and Harrington*, 1988; *Trouet et al.*, 2009; *Abatzoglou and Kolden*, 2013]. However, there is increased understanding of linkages between wildfire synchrony over regional scales and interannual to multidecadal patterns in climate variation influenced by global teleconnections such as the El Niño–Southern Oscillation (ENSO) and other coupled ocean-atmosphere temperature and pressure patterns [*Swetnam and Betancourt*, 1990; *Kitzberger et al.*, 2001, 2007; *Trouet et al.*, 2010; *Labosier et al.*, 2015]. These patterns affect regional droughts that, in turn, affect local patterns in fuel moisture and lightning ignitions.

Wildfire records in many regions of the world are generally too short or incomplete to adequately assess long-term effects of synoptic climate forcings on wildfires [*Swetnam and Brown*, 2010]. Many areas also have experienced disruptions in natural fire occurrence through all or portions of the 20th and 21st centuries because of fire suppression activities or intensive livestock grazing, logging, or other land use activities that changed characteristic fuel amount, structure, and continuity [e.g., *Hessl et al.*, 2016]. Thus, much of our current understanding of long-term fire-climate linkages has come about through comparison of multicentury wildfire chronologies derived from fire scars recorded in annual tree ring series with independently derived tree ring-based climate reconstructions [*Trouet et al.*, 2010; *Falk et al.*, 2011]. For example, evidence from western North America has shown how contingent states of ENSO, the Pacific Decadal Oscillation (PDO), and the Atlantic Multidecadal Oscillation (AMO) influenced regional spatial and temporal variability
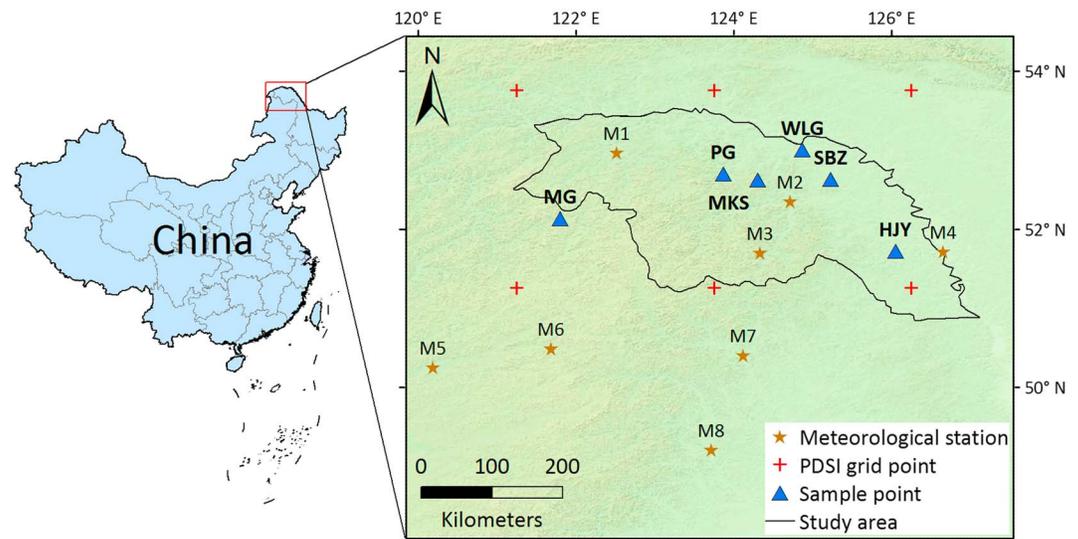
Figure 1. Locations of fire scar collections in northeast China (blue triangles) within area of Daxing'an Mountains. Red crosses are PDSI grid points [*Dai et al.*, 2004] used in SEA with regional wildfire index. Yellow pentagrams are the locations of meteorological station sites.

in multidecadal drought frequencies [*McCabe et al.*, 2004] that, in turn, contributed to increase wildfire synchrony across individual mountain ranges [*Brown*, 2006; *Sibold and Veblen*, 2006] and at subcontinental scales [*Trouet et al.*, 2006, 2009, 2010; *Kitzberger et al.*, 2007]. Understanding how quasiperiodic variations in ocean-atmosphere phenomena affect interannual to multidecadal climate variation holds promise for probabilistic drought and wildfire forecasts months to perhaps years in advance [*Falk et al.*, 2011; *Owen et al.*, 2012] and contributes to more accurate modeling of climate change impacts on wildfires and ecosystems in coming decades [*Liu et al.*, 2014].

Whereas the development and interpretation of century-length wildfire chronologies has evolved steadily for certain regions such as western North America, such chronologies do not exist for other regions, including northeastern China. Yet wildfire hazard is projected to increase with increasing temperatures in the coming century in regions of Siberia and northeastern China [*Kasischke*, 2000; *Liu et al.*, 2012] and an improved understanding of fire history is urgently needed for these regions. Furthermore, the influence of atmospheric circulation patterns on climate in northeast China is only beginning to be explored [*Dai et al.*, 2004; *X. Wang et al.*, 2011; *Linderholm et al.*, 2013; *Qian et al.*, 2014] and very little is known about teleconnection relations with wildfires. Here we construct multicentury wildfire histories from fire scars recorded in Dahurian larch (*Larix gmelinii*) trees found at six sites across the Daxing'an Mountains in northeast China (Figure 1 and Table S1 in the supporting information). Our goals are (1) to reconstruct local and regional wildfire dates and relative spatial extent in northeast China over the last ~250 years and (2) to assess climatic forcings of wildfires across this region. We combined wildfire dates recorded simultaneously in at least two of the six sites to develop a regional wildfire index from 1774 to 2010 A.D. that we compare to regional droughts and global climate teleconnections. Based on results from similar studies from other regions [*Falk et al.*, 2010], we hypothesize that regional synchrony in wildfire occurrence was driven by regional climate patterns that overrode smaller-scale effects, such as human land use or local changes in fuel structure. We also examine the influence of large-scale climate oscillation patterns on local climatology over the existing instrumental period.

2. Materials and Methods

2.1. Study Area

The Daxing'an Mountains are a unique boreal forest region in China located at the southern limit of a discontinuous permafrost zone [*Xu*, 1998]. Annual mean temperatures vary from −2 to −4°C. Mean annual precipitation ranges between 350 and 500 mm with >60% occurring from June to August [*Zhou*, 1991; *Abaimov et al.*, 2000; *Shi et al.*, 2000]. Winters are generally dry, and peak fire season occurs in the arid foresummer from March to June, although fires can also occur during extreme summer drought and into the fall. The ignition

source of most wildfires in Daxing'an Mountains before 1949 is mainly from lightning, while the man-made fires increased gradually after 1949 [*Xu*, 1998].

2.2. Wildfire Data

Fire-scarred cross sections were collected in the summer of 2010 at six sites in the Daxing'an Mountains in northeast China (Figure 1 and Table S1 in the supporting information). Cross sections were prepared and sanded to be able to see wood cell structure under 7X to 30X magnification with a stereo microscope. Tree ring series on cross sections were then crossdated against locally developed master chronologies for each site [*X.-C Wang et al.*, 2011] using both visual and skeleton plot crossdating methods [*Speer*, 2010]. The year and season of occurrence of fire scars recorded on individual trees were assigned and compiled into fire chronologies for each site using the program FHX2 [*Grissino-Mayer*, 2001]. We then compiled a regional wildfire index that consists of site level fire scar dates (defined as fire dates recorded on greater than or equal to two trees at an individual site) recorded at greater than or equal to two sites to examine climate relations with regional wildfire occurrence over the past two+ centuries.

2.3. Climate Data

We first derived a regional drought index from a set of gridded (2.5° latitude × 2.5° longitude) April–October Palmer Drought Severity Indices (PDSI) developed from instrumental records (1901–2014) across China and northeast Asia [*Dai et al.*, 2004]. Our regional drought index includes average annual values for six grid points centered over northeast China (Figure 1). We compared the regional wildfire index to this seasonal drought index both graphically and using superposed epoch analyses (SEA) over the period of overlap (1901–2014 C. E. (Common Era)), which included 15 regional wildfire dates. We used the program FHAES (Fire History Analysis and Exploration System) for SEA [*Brewer et al.*, 2014]. Significant climate anomalies in SEA were determined using bootstrapped confidence intervals based on average annual climate values with the same number of years in the regional wildfire index data set.

In addition to instrumental PDSI [*Dai et al.*, 2004], we compared regional wildfire dates to the Monsoon Asia Drought Atlas version 2 (MADA), a reconstruction of summer (June–August) PDSI across Asia (1300–2005) [*Cook et al.*, 2010]. The MADA reconstructions are gridded on the same locations as the instrumental PDSI [*Dai et al.*, 2004] (Figure 1). However, we did not find any significant relations with MADA grid points in the Daxing'an Mountains, we suspect, because of either different seasons of analysis (April to October in the instrumental data versus June to August in the MADA reconstruction) or the general lack of tree ring chronologies in northeast China for MADA grid point reconstruction.

We then compared regional wildfire dates to four proxy-based reconstructions of three atmospheric circulation patterns: two tree ring-based reconstructions of ENSO (Winter SOI: 1706–1977; [*Stahle et al.*, 1998]) and Winter Niño3 index (1408–1978; [*Cook et al.*, 2009]); a tree ring-based reconstruction of Annual PDO (standardized leading principal component of monthly SST anomalies in the Pacific north of 20°N; 1700–1979; [*D'Arrigo et al.*, 2001]); and a reconstruction of the North Atlantic Oscillation (NAO; calculated as the standardized difference between sea level pressure over the Azores and Iceland; April–October 1500–2001; [*Luterbacher*, 2001]). We recognize that there are issues with available PDO reconstructions [*Kipfmueller et al.*, 2012] but believe our results support using the reconstruction [*D'Arrigo et al.*, 2001] as robust in relation to wildfires in northeast China. We use SOI and Niño3 as proxies for ENSO as these have proven to be robust indicators of the ENSO teleconnection in fire-climate analyses for North America [e.g., *Brown*, 2006; *Sibold and Veblen*, 2006; *Kitzberger et al.*, 2007]. There are 30 regional wildfire dates that overlap with the SOI and PDO reconstructions and 31 that overlap with the Niño3 and NAO reconstructions. We also tested relationships between regional wildfire dates and contingent combinations of the Southern Oscillation Index (SOI), PDO, and NAO reconstructions using a chi-square contingency analysis calculated in R.

2.4. Climate Teleconnections

We extracted monthly climate parameters (precipitation anomalies, temperature anomalies, and relative humidity) from eight meteorological stations (Figure 1 and Table S2) located near the fire history sites, then we averaged the three climate parameters (anomalies were calculated from 1957 to 2009 average) of eight stations to explore potential linkages between local climatology and atmospheric circulation patterns as indicated by the fire-climate analysis. We used Pearson's correlations to compare local seasonal climate
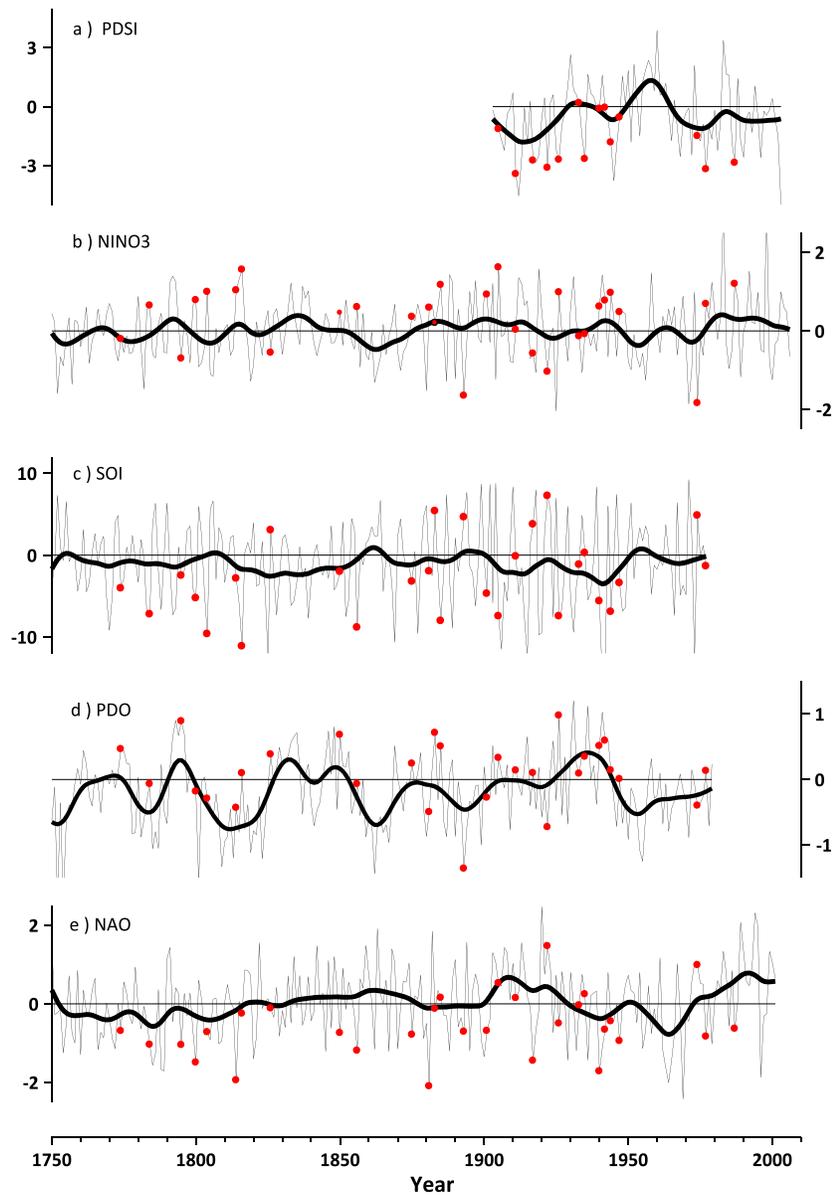
Figure 2. Time series of (a) instrumental PDSI and (b) reconstructed Niño3, (c) SOI, (d) PDO, and (e) NAO with regional wildfires marked at the dates they occurred (red circles). Heavy lines in each plot are 20 year cubic spline smoothing curves; light straight lines are time series means.

conditions to instrumental circulation series (SOI [*Allan et al.*, 1991], NAO [*Jones et al.*, 1997], and PDO [*Mantua et al.*, 1997]) over a common period from 1957 to 2009.

3. Results

3.1. Wildfire-Climate History

We were able to crossdate 207 fire-scarred trees from the six sites sampled in the Daxing'an Mountains, with individual wildfire dates extending from 1693 to 2007 (Figure S1). Wildfires were frequent occurrences in all sites, although there was a decline in both local and regional wildfire frequency after 1947. We identified 31 regional wildfires (recorded at two or more sites) from the first recorded in 1774 to the last in 1987 (Figure S1). Regional wildfires occurred on average every 7 years from 1774 to 1947 (Table S3). We did not calculate fire frequency after 1947 because of the obvious change in wildfire frequency after this date. Only three regional
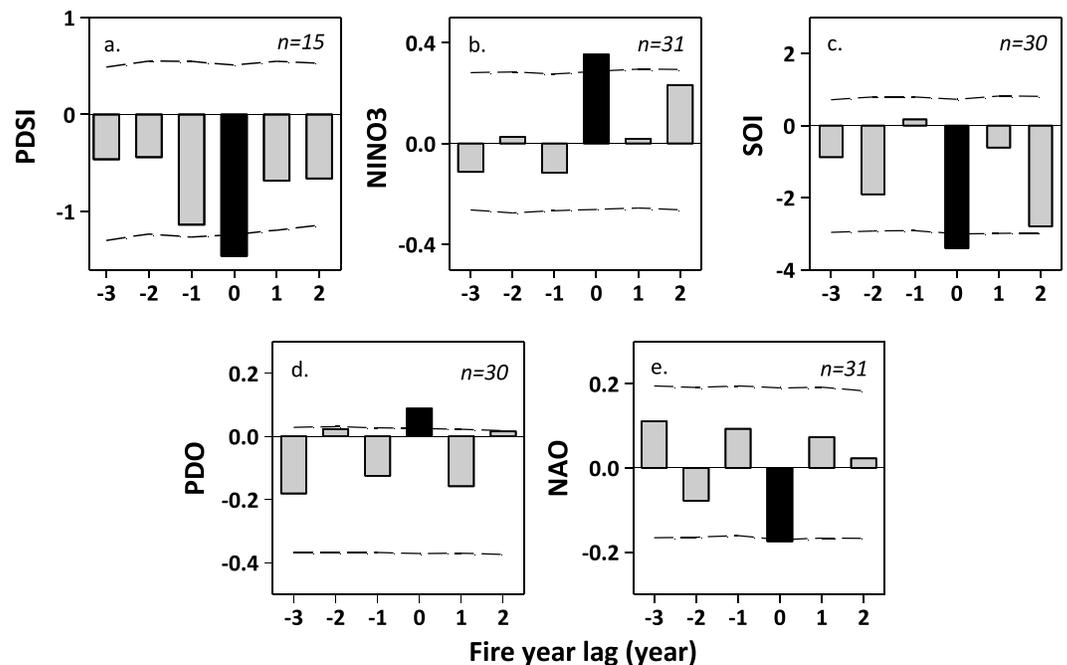
Figure 3. Superposed epoch analyses of instrumental (PDSI; 1901–2010) and reconstructed (Niño3, SOI, PDO, and NAO; 1774–2010) annual climate anomalies with regional wildfire years in northeastern China. The analysis window includes 3 years before and 2 years after each fire year (year "0"). Fire years are defined as years when at least two of the six sites burned (Figure 2). Black bars mark statistically significant departures ($p < 0.05$; dashed lines) from mean conditions.

wildfires were recorded after 1947: in 1974, 1977, and 1987. Fire scars were generally recorded as dormant (before growth began for the year) or early in the ring for any 1 year.

Regional wildfires exhibit consistent and significant relationships with regional drought during the twentieth century and with atmospheric circulation patterns since 1774 (Figures 2 and 3). Regional wildfires typically occurred during years of low PDSI (Figures 2a and 3a), El Niño years (positive Niño3 (Figures 2b and 3b) and negative SOI (Figures 2c and 3c)), positive phases of the PDO (Figures 2d and 3d), and negative phases of the NAO (Figures 2e and 3e). We did not find any lagged relationships in SEA with any of the climate indices, indicating that prior fuel buildup is not necessary for regional wildfires to occur [e.g., *Brown and Wu*, 2005]. We also find in the chi-square contingency test of expected versus observed wildfire dates that contingent combinations of years when El Niño, positive PDO, and negative NAO occurred led to more wildfires than expected if wildfire occurred by chance (Table 1).

3.2. Climate Teleconnections

Correlations between seasonal meteorological station parameters and large-scale climate oscillations over the common period 1957–2009 support linkages seen in the historical wildfire data (Table 2). Spring SOI and relative humidity were positively correlated (0.28; $p < 0.05$, $n = 53$), as were previous winter PDO and temperature anomalies (0.28; $p < 0.05$, $n = 53$). NAO was negatively correlated with spring temperature anomalies (−0.41; $p < 0.01$, $n = 53$) and positively correlated with precipitation anomalies (0.39; $p < 0.01$, $n = 53$) and relative humidity (0.33; $p < 0.05$, $n = 53$) in summer.

4. Discussion

Wildfires were common occurrences in the Daxing'an Mountains of northeastern China for at least two centuries before 1947 (Figure S1 and Table S3). Wildfires occurred most often as spring fires before tree ring growth began for each year. Early season fires are common both in wildfire records for this area [*Xu*, 1998; *Chang et al.*, 2008] and in nearby regions of northeast Mongolia [*Hessl et al.*, 2016]. Regional wildfires (recorded in at least two of the six sites) occurred on average every 7 years from 1774 to 1947, with a marked decline in both site level and regional fire occurrence in the latter half of the twentieth century (Figure S1). We

Table 1. Expected Versus Observed Numbers of 30 Regional Wildfire Years (1774–1977) for Eight Phase Combinations of Reconstructed SOI, PDO, and NAO[a]

Case	SOI− PDO− NAO−	SOI− PDO− NAO+	SOI− PDO+ NAO−	SOI+ PDO− NAO−	SOI+ PDO+ NAO+	SOI+ PDO+ NAO−	SOI+ PDO− NAO+	SOI− PDO+ NAO+
Observed	6	2	**12**	1	3	1	2	3
Expected	4.71	3.38	**5**	4.41	2.21	0.74	5.29	4.26
P value	0.516	0.425	**0.000**	0.079	0.579	0.755	0.115	0.508

[a]Bold observed number of fires is significantly different from random expectation in chi-square test ($X^2 = 16.16$; d$f = 7$, $P = 0.02$). Negative SOI represents El Niño conditions. Contingency analysis using Niño3 instead of SOI as a proxy for ENSO showed similar results.

also run a SEA and a contingency analysis for the period 1774–1949 C.E. for all indices and found similar results (Figure S3 and Table S4). The different fire-PDSI SEAs results (1901–2010) with versus without the post-1949 period (1901–1949) may be due to the short time series and more fire events.

Firefighting efforts were nationalized after the founding of the People's Republic of China in 1949, with increased funding and manpower directed to total fire exclusion in forested regions of the country [*Xu*, 1998; *Chang et al.*, 2008]. These efforts appear to have been mostly effective, with many fewer fire scars recorded in trees after 1947. However, regional wildfires are again present in the record in 1974 and 1977 and culminate most recently in the infamous Black Dragon (Heilongjiang) Fire that started in May 1987. The Black Dragon Fire burned ~73,000 km^2 on both sides of the Heilongjiang (Amur) River that marks the northern boundary between China and Russia [*Salisbury*, 1989]. This was arguably the largest single wildfire in recorded history and caused the deaths of over 200 people in China with an additional 56,000 displaced. The fire burned mostly unchecked in Russia, but was heavily fought by firefighters, troops, and forestry workers in China.

Regional wildfires were consistently and significantly associated with regional droughts, positive phases of ENSO and PDO, and negative phases of NAO (Figures 2, 3, and S2 and Table 1). Similar to patterns seen in fire scar records across North America, contingent combinations of atmospheric circulation patterns result in recognizable and consistent patterns in both droughts and wildfires [*Brown*, 2006; *Sibold and Veblen*, 2006; *Trouet et al.*, 2006, 2009, 2010; *Kitzberger et al.*, 2007]. In northeastern China, teleconnection interactions can be related to more regional wildfires than expected by chance alone (Table 1). Correlations between meteorological station climate parameters and climate modes (Table 2) also show significant linkages between atmospheric circulation patterns and droughts that contribute to wildfire occurrence. The contingent combination of +ENSO/+PDO/−NAO seen in the historical regional fire years is linked to low humidity, low precipitation, and high temperature during or before late spring fire seasons in meteorological records (Table 2). And the climate mechanism between the NAO and drought in NE China may possibly be associated with changes in the position of the Jet stream, which is linked with local climate in northeast Asia [*Liao et al.*,

Table 2. Pearson Correlation Coefficients Between the Large-Scale Climate Oscillations and Local Climate Parameters

		Precipitation Anomalies				Temperature Anomalies				Relative Humidity			
		Winter	Spring	Summer	Autumn	Winter	Spring	Summer	Autumn	Winter	Spring	Summer	Autumn
SOI	Winter	0.03	0.11	−0.16	−0.18	−0.07	0.06	−0.05	0.01	0.00	−0.07	−0.09	−0.07
	Spring		0.16	−0.25	0.04		−0.06	−0.01	−0.04		0.28*	−0.10	0.03
	Summer			−0.22	0.16			0.07	0.12			−0.05	0.09
	Autumn				0.22				0.16				0.03
PDO	Winter	0.05	0.03	−0.05	0.05	0.28*	0.25	0.16	0.22	−0.22	−0.09	−0.09	−0.07
	Spring		0.01	0.19	−0.12		0.12	0.04	0.18		0.04	0.11	−0.22
	Summer			0.14	−0.18			−0.07	0.03			0.09	−0.16
	Autumn				−0.16				−0.26				0.02
NAO	Winter	0.08	0.26	0.12	0.13	−0.01	0.02	0.26	0.13	−0.09	0.22	0.10	0.05
	Spring		−0.10	−0.04	0.04		−0.41**	−0.19	−0.29*		−0.02	0.08	0.12
	Summer			0.39**	−0.13			−0.13	0.08			0.33*	0.08
	Autumn				0.06				−0.20				0.23

*$P < 0.05$,
**$P < 0.01$. Winter (DJFM), Spring (AMJ), Summer (JA), and Autumn (SON).

2004]. These results add to a growing understanding of relationships between teleconnections and precipitation and other climate patterns across China [*Li et al.*, 2004, 2005; *D'Arrigo and Wilson*, 2006; *Qian and Qin*, 2008; *Qian et al.*, 2014] and support our finding of an indirect linkage between wildfires and Pacific and Atlantic Ocean teleconnections through direct teleconnection effects on drought occurrence in this area of the world.

Identifying atmospheric circulation effects on wildfires and droughts in northeastern China adds to a growing understanding of global wildfire-teleconnection linkages and will improve predictions of how wildfire and drought regimes may respond to changing future climate conditions [e.g., *Bowman et al.*, 2009; *Brown*, 2006; *Sibold and Veblen*, 2006; *Trouet et al.*, 2006, 2009, 2010; *Kitzberger et al.*, 2007]. Our results have implications for forecasting wildfire and drought dynamics both during coming fire seasons in China and under future climate change. For example, this spring saw ENSO in a "super El Niño" phase [*National Weather Service Climate Prediction Center* (*NWS CPC*), 2015; *Schiermeier*, 2015], with PDO also trending positive [*NWS CPC*, 2015]. The recent spring wildfire season in early 2016 in northeastern China was one of the worst in several years, with four large wildfires reported in May 2016 in the Daxing'an Mountains with more than 4000 people involved in firefighting efforts [*China*, 2016]. In contrast, however, NAO has been trending positive since 2014 [*NWS CPC*, 2015], which may have helped to lessen the risk of regional wildfires in summer 2016.

Our wildfire history also has important implications for fire and forest management in the Daxing'an Mountains and adjacent regions. Frequent, low-intensity wildfires would have tended to remove small trees and consume dead wood and needle litter while having little effect on mature trees and overall forest structures [e.g., *Brown and Wu*, 2005]. Fire suppression since 1949 has likely contributed to increased fuel loads and denser forest canopies, which may, in turn, have contributed to more severe fire behavior, tree mortality, and more extensive burning during recent wildfires, such as the Black Dragon Fire in 1987. This scenario has been postulated by other researchers working in this region [*Chang et al.*, 2007; *Liu et al.*, 2012]. The situation in northeastern China likely shares characteristics of frequent-fire forests of western North America, where fire exclusion through the twentieth century has led to increased burn severity during recent wildfires and subsequently more severe impacts on natural resources and human infrastructure [*Stephens and Ruth*, 2005; *Rocca et al.*, 2014]. A history of fire suppression starting in the latter twentieth century coupled with climate change will most likely contribute to increased wildfire occurrences and possibly severities in coming years in northeastern China. Management policies could be implemented to incorporate better understanding of fire-climate relationships in fuel reduction treatments to help mitigate these combined effects in the future. For example, prescribed fires could be implemented in contingent scenarios of −ENSO/−PDO/+NAO during which local weather would be expected to be relatively more moderate, while implementing total fire exclusion during years with contingent combinations of +ENSO/+PDO/−NAO during which past regional wildfires occurred.

5. Conclusion

Wildfire history from the Daxing'an Mountains in northeast China reconstructed from fire scars has identified 31 regional wildfires from 1774 to 1987. Wildfires were common occurrences prior to a period of relatively effective fire suppression initiated after 1949. Regional wildfires occurred predominately during drought years, which also occurred during El Niños, positive phases of PDO, and negative phases of NAO. The influence of these atmospheric circulation patterns on regional wildfire regimes is supported by strong and consistent links with local climate parameters over the instrumental period. The wildfire history provides a unique foundation for understanding the longer-term role of wildfires in the ecology and management of Dahurian larch forests of this region and for providing insights into the role of atmospheric circulation patterns in climate forcing across China and eastern Asia.

References

Abaimov, A. P., O. A. Zyryanova, S. G. Prokushkin, T. Koike, and Y. Matsuura (2000), Forest ecosystems of the cryolithic zone of Siberia: Regional features, mechanisms of stability and pyrogenic changes, *Eurasian J. For. Res.*, 1, 1–10.

Abatzoglou, J. T., and C. A. Kolden (2013), Relationships between climate and macroscale area burned in the western United States, *Int. J. Wildl. Fire*, 22(7), 1003–1020, doi:10.1071/WF13019.

Abatzoglou, J. T., and A. P. Williams (2016), Impact of anthropogenic climate change on wildfire across western US forests, *Proc. Natl. Acad. Sci. U.S.A.*, 113(42), 11,770–11,775, doi:10.1073/pnas.1607171113.

Allan, R. J., N. Nicholls, P. D. Jones, and I. J. Butterworth (1991), A further extension of the Tahiti-Darwin SOI, early ENSO events and Darwin pressure, *J. Clim.*, *4*, 743–752, doi:10.1175/1520-0442(1991)004<0743:AFEOTT>2.0.CO;2.

Bowman, D. M. J. S., et al. (2009), Fire in the Earth system, *Science*, *324*, 481–484, doi:10.1126/science.1163886.

Brewer, P. W., M. E. Velásquez, E. K. Sutherland, and D. A. Falk (2014), Fire History Analysis and Exploration System (FHAES).

Brown, P. M. (2006), Climate effects on fire regimes and tree recruitment in Black Hills ponderosa pine forests, *Ecology*, *87*(10), 2500–2510, doi:10.1890/0012-9658(2006)87[2500:CEOFRA]2.0.CO;2.

Brown, P. M., and R. Wu (2005), Climate and disturbance forcing of episodic tree recruitment in a southwestern ponderosa pine landscape, *Ecology*, *86*(11), 3030–3038, doi:10.1890/05-0034.

Chang, Y., H. S. He, Y. Hu, R. Bu, and X. Li (2008), Historic and current fire regimes in the Great Xing'an Mountains, northeastern China: Implications for long-term forest management, *For. Ecol. Manage.*, *254*(3), 445–453, doi:10.1016/j.foreco.2007.04.050.

Chang, Y., H. S. He, I. Bishop, Y. Hu, R. Bu, and C. L. Xu (2007), Long-term forest landscape responses to fire exclusion in the Great Xing'an Mountains, China, *Int. J. Wildl. Fire*, *16*, 34–44.

China, S. F. A. (2016), Urgent warnings for the high risk of wildfire in Daxing'an Mountain, *State For. Adm. People's Repub. China*. [Available at. [Available at http://www.forestry.gov.cn/main/3562/content-873855.html.]

Cook, E. R., K. J. Anchukaitis, B. M. Buckley, R. D. D'Arrigo, G. C. Jacoby, and W. E. Wright (2010), Asian monsoon failure and megadrought during the last millennium, *Science*, *328*(5977), 486–9, doi:10.1126/science.1185188.

Cook, E. R., et al. (2009), Tree Ring 500 year ENSO index reconstructions, *IGBP PAGES/World Data Cent. Paleoclimatology Data Contrib. Ser. 2009-105.(NOAA/NCDC Paleoclimatology Program)*.

D'Arrigo, R., and R. Wilson (2006), On the Asian expression of the PDO, *Int. J. Climatol.*, *26*(12), 1607–1617, doi:10.1002/joc.1326.

D'Arrigo, R., R. Villalba, and G. Wiles (2001), Tree-ring estimates of Pacific decadal climate variability, *Clim. Dyn.*, *18*(3–4), 219–224, doi:10.1007/s003820100177.

Dai, A., K. E. Trenberth, and T. Qian (2004), A global dataset of Palmer Drought severity index for 1870–2002: Relationship with soil moisture and effects of surface warming, *J. Hydrometeorol.*, *5*(6), 1117–1130, doi:10.1175/JHM-386.1.

Falk, D. A., E. K. Heyerdahl, P. M. Brown, T. W. Swetnam, E. K. Sutherland, Z. Gedalof, L. Yocom, and T. J. Brown (2010), Fire and climate variation in western North America from fire-scar and tree-ring networks, *PAGES News*, *18*(2), 70–72, doi:10.1029/2010GL043706.For.

Falk, D. A., E. K. Heyerdahl, P. M. Brown, C. Farris, P. Z. Fulé, D. McKenzie, T. W. Swetnam, A. H. Taylor, and M. L. Van Horne (2011), Multi-scale controls of historical forest-fire regimes: New insights from fire-scar networks, *Front. Ecol. Environ.*, *9*(8), 446–454, doi:10.1890/100052.

Flannigan, M. D., and J. B. Harrington (1988), A study of the relation of meteorological variable to monthly provincial area burned by wildfire in Canada (1953-80), *J. Appl. Meteorol.*, *27*, 441–452.

Grissino-Mayer, H. (2001), FHX2-software for analyzing temporal and spatial patterns in fire regimes from tree rings, *Tree-Ring Res.*, *57*(1), 115–124.

Hessl, A. E., P. M. Brown, O. Byambasuren, S. Cockrell, C. Leland, E. R. Cook, N. Nachin, N. Pederson, T. Saladyga, and B. Suran (2016), Fire and climate in Mongolia (1532–2010 Common Era), *Geophys. Res. Lett.*, *43*, 6519–6527, doi:10.1002/2016GL069059.

Jolly, W. M., M. A. Cochrane, P. H. Freeborn, Z. A. Holden, T. J. Brown, G. J. Williamson, and D. M. J. S. Bowman (2015), Climate-induced variations in global wildfire danger from 1979 to 2013, *Nat. Commun.*, *6*, 7537, doi:10.1038/ncomms8537.

Jones, P. D., T. Jonsson, and D. Wheeler (1997), Extension to the North Atlantic oscillation using early instrumental pressure observations from Gibraltar and south-west Iceland, *Int. J. Climatol.*, *17*(13), 1433–1450, doi:10.1002/(SICI)1097-0088(19971115)17:13<1433::AID-JOC203>3.0.CO;2-P.

Kasischke, E. (2000), in *Fire, Climate Change, and Carbon Cycling in the Boreal Forest. Ecological Studies*, edited by B. Stocks, Springer, Berlin.

Kipfmueller, K. F., E. R. Larson, and S. S. George (2012), Does proxy uncertainty affect the relations inferred between the Pacific Decadal Oscillation and wildfire activity in the western United States?, *Geophys. Res. Lett.*, *39*, L04703, doi:10.1029/2011GL050645.

Kitzberger, T., T. W. Swetnam, and T. T. Veblen (2001), Inter-hemispheric synchrony of forest fires and the El Niño–Southern Oscillation, *Global Ecol. Biogeogr.*, *10*(3), 315–326, doi:10.1046/j.1466-822X.2001.00234.x.

Kitzberger, T., P. M. Brown, E. K. Heyerdahl, T. W. Swetnam, and T. T. Veblen (2007), Contingent Pacific-Atlantic Ocean influence on multi-century wildfire synchrony over western North America, *Proc. Natl. Acad. Sci. U.S.A.*, *104*(2), 543–548, doi:10.1073/pnas.0606078104.

Labosier, C. F., O. W. Frauenfeld, S. M. Quiring, and C. W. Lafon (2015), Weather type classification of wildfire ignitions in the central Gulf Coast, United States, *Int. J. Climatol.*, *35*, 2620–2634, doi:10.1002/joc.4160.

Li, C., J. He, and J. Zhu (2004), A review of decadal/interdecadal climate variation studies in China, *Adv. Atmos. Sci.*, *21*(3), 425–436, doi:10.1007/BF02915569.

Li, Q., S. Yang, V. E. Kousky, R. W. Higgins, K. M. Lau, and P. Xie (2005), Features of cross-pacific climate shown in the variability of China and US precipitation, *Int. J. Climatol.*, *25*(13), 1675–1696, doi:10.1002/joc.1271.

Liao, Q., S. Gao, H. Wang, and S. Tao (2004), Anomalies of the extratropical westerly Jet in the north hemisphere and their impacts on east Asian summer monsoon climate anomalies, *Chin. J. Geophys.*, *47*, 10–18.

Linderholm, H. W., A. Seim, T. Ou, J. H. Jeong, Y. Liu, X. Wang, G. Bao, and C. Folland (2013), Exploring teleconnections between the summer NAO (SNAO) and climate in East Asia over the last four centuries—A tree-ring perspective, *Dendrochronologia*, *31*(4), 297–310, doi:10.1016/j.dendro.2012.08.004.

Liu, Y., J. Stanturf, and S. Goodrick (2010), Trends in global wildfire potential in a changing climate, *For. Ecol. Manage.*, *259*(4), 685–697, doi:10.1016/j.foreco.2009.09.002.

Liu, Y., S. Goodrick, and W. Heilman (2014), Wildland fire emissions, carbon, and climate: Wildfire-climate interactions, *For. Ecol. Manage.*, *317*, 80–96, doi:10.1016/j.foreco.2013.02.020.

Liu, Z., J. Yang, Y. Chang, P. J. Weisberg, and H. S. He (2012), Spatial patterns and drivers of fire occurrence and its future trend under climate change in a boreal forest of Northeast China, *Global Change Biol.*, *18*, 2041–2056, doi:10.1111/j.1365-2486.2012.02649.x.

Luterbacher, J. (2001), Extending North Atlantic Oscillation reconstructions back to 1500, *Atmos. Sci. Lett.*, *2*(1–4), 114–124, doi:10.1006/asle.2001.0044.

Mantua, N. J., S. R. Hare, Y. Zhang, J. M. Wallace, and R. C. Francis (1997), A Pacific interdecadal climate oscillation with impacts on salmon production, *Bull. Am. Meteorol. Soc.*, *78*(6), 1069–1079, doi:10.1175/1520-0477(1997)078<1069:APICOW>2.0.CO;2.

McCabe, G. J., M. A. Palecki, and J. L. Betancourt (2004), Pacific and Atlantic Ocean influences on multidecadal drought frequency in the United States, *Proc. Natl. Acad. Sci. U.S.A.*, *101*(12), 4136–4141, doi:10.1073/pnas.0306738101.

Moritz, M. A., et al. (2014), Learning to coexist with wildfire, *Nature*, *515*(7525), 58–66, doi:10.1038/nature13946.

National Weather Service Climate Prediction Center (NWS CPC) (2015), NCEP Global Ocean Data Assimilation System (GODAS).

Owen, G., J. D. McLeod, C. A. Kolden, D. B. Ferguson, and T. J. Brown (2012), Wildfire management and forecasting fire potential: The roles of climate information and social networks in the southwest United States, *Weather Clim. Soc.*, *4*(2), 90–102, doi:10.1175/WCAS-D-11-00038.1.

Qian, C., J.-Y. Yu, and G. Chen (2014), Decadal summer drought frequency in China: The increasing influence of the Atlantic Multi-decadal Oscillation, *Environ. Res. Lett.*, *9*(12), 124004, doi:10.1088/1748-9326/9/12/124004.

Qian, W. H., and A. Qin (2008), Precipitation division and climate shift in China from 1960 to 2000, *Theor. Appl. Climatol.*, *93*(1–2), 1–17, doi:10.1007/s00704-007-0330-4.

Rocca, M. E., P. M. Brown, L. H. MacDonald, and C. M. Carrico (2014), Climate change impacts on fire regimes and key ecosystem services in Rocky Mountain forests, *For. Ecol. Manage.*, *327*, 290–305, doi:10.1016/j.foreco.2014.04.005.

Salisbury, H. E. (1989), *The Great Black Dragon Fire: A Chinese Inferno*, Little, Brown, Boston, Mass.

Schiermeier, Q. (2015), Hunting the Godzilla El Niño, *Nature*, *526*, 490–491, doi:10.1038/526490a.

Shi, F., Y. Zu, K. Suzuki, S. Yamamoto, M. Nomura, and K. Sasa (2000), Effects of site preparation on the regeneration of larch dominant forests after a forest fire in the Daxinganling Mountain region, Northeast China, *Eurasian J. For. Res.*, *1*, 11–17.

Sibold, J. S., and T. T. Veblen (2006), Relationships of subalpine forest fires in the Colorado Front Range with interannual and multidecadal-scale climatic variation, *J. Biogeogr.*, *33*(5), 833–842, doi:10.1111/j.1365-2699.2006.01456.x.

Speer, J. (2010), *Fundamentals of Tree-Ring Research*, Univ. Ariz. Press, Tucson.

Stahle, D. S., et al. (1998), Experimental dendroclimatic reconstruction of the southern oscillation, *Bull. Am. Meteorol. Soc.*, *79*(10), 2137–2152, doi:10.1175/1520-0477(1998)079<2137:EDROTS>2.0.CO;2.

Stephens, S. L., and L. W. Ruth (2005), Federal forest-fire policy in the United States, *Ecol. Appl.*, *15*(2), 532–542, doi:10.1890/04-0545.

Swetnam, T. W., and J. L. Betancourt (1990), Fire-southern oscillation relations in the Southwestern United States, *Science*, *249*, 1017–1020.

Swetnam, T. W., and P. M. Brown (2010), In *Dendroclimatology: Progress and Prospects*, edited by M. K. Hughes, H. F. Diaz, and T. W. Swetnam, Springer, New York.

Trouet, V., A. H. Taylor, A. M. Carleton, and C. N. Skinner (2006), Fire-climate interaction in forests of the American Pacific coast, *Geophys. Res. Lett.*, *33*, L18704, doi:10.1029/2006GL027502.

Trouet, V., A. H. Taylor, A. M. Carleton, and C. N. Skinner (2009), Interannual variations in fire weather, fire extent, and synoptic-scale circulation patterns in northern California and Oregon, *Theor. Appl. Climatol.*, *95*(3–4), 349–360, doi:10.1007/s00704-008-0012-x.

Trouet, V., A. H. Taylor, E. R. Wahl, C. N. Skinner, and S. L. Stephens (2010), Fire-climate interactions in the American West since 1400 CE, *Geophys. Res. Lett.*, *37*, L04702, doi:10.1029/2009GL041695.

Wang, X., P. M. Brown, Y. Zhang, and L. Song (2011), Imprint of the Atlantic multidecadal oscillation on tree-ring widths in Northeastern Asia since 1568, *PLoS One*, *6*(7), 1–6, doi:10.1371/journal.pone.0022740.

Wang, X.-C., L.-P. Song, and Y.-D. Zhang (2011), Climate-tree growth relationships of *Pinus sylvestris* var. *mongolica* in the northern Daxing'an Mountains, China, *Chin. J. Plant Ecol.*, *35*(3), 294–302, doi:10.3724/SP.J.1258.2011.00294.

Westerling, A. L., H. G. Hidalgo, D. R. Cayan, and T. W. Swetnam (2006), Warming and earlier spring increase western U.S. forest wildfire activity, *Science*, *313*(5789), 940–943, doi:10.1126/science.1128834.

Xu, H. (1998), *Daxing'an Mountain Forest in China*, Science Press, Beijing.

Zhou, Y. (1991), *Vegetation in the Great Xing'an Mountains of China*, Science Press, Beijing.